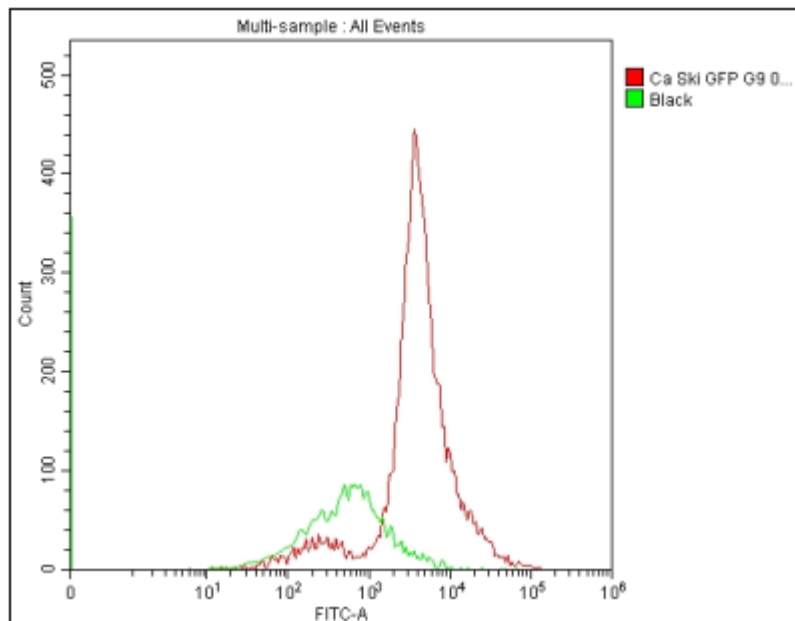


SUPPLEMENTARY MATERIALS

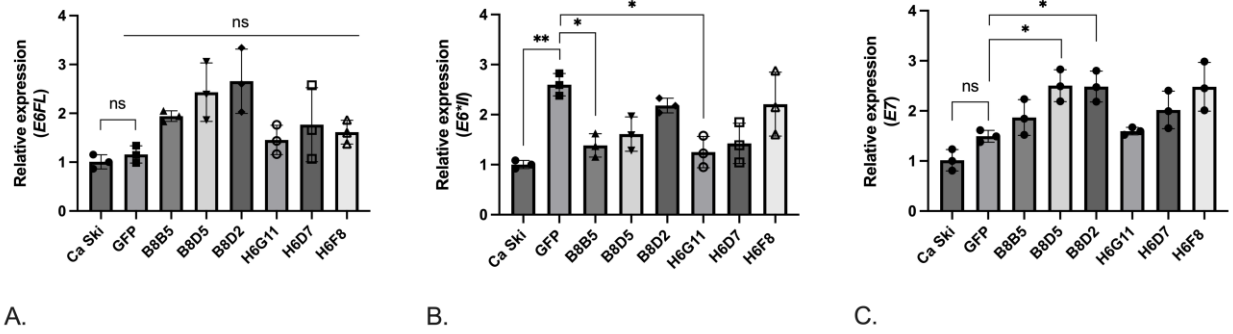
Supplementary Table S1. List of primers used in the experiments. Fw – forward, rev – reverse.

Target sequence (gene)	Direction	Primer sequence
<i>GAPDH</i>	fw	5'-CAACGGATTTGGTCGTATTGG-3'
	rev	5'-GCAACAATATCCACTTTACCAGAGTTAA-3'
<i>GUSB</i>	fw	5'-CGTGGTTGGAGAGCTCATTTGGAA-3'
	rev	5'-ATTCCCCAGCACTCTCGTCGGT-3'
<i>Reverse transcriptase of HIV-1 FSU_A strain (RT_A)</i>	fw	5'-CTGGAGCTTGCTGAGAATAGAG-3'
	rev	5'-CACTGGTCCTGTCCTTGTTT-3'
<i>E6FL</i>	fw	5'-AAGTTAACCACAGTTATGC-3'
	rev	5'-TGTTCTAATGTTGTTCCAT-3'
<i>E6*I</i>	fw	5'-AGGAGCGACCCAGAAAGTTA-3'
	rev	5'-GCTTTTGACAGTTAATACACCTCAC-3'
<i>E6*II</i>	fw	5'-AGGAGCGACCCAGAAAGTTA-3'
	rev	5'-TACGTGTTCTTATGATCTCAGGTC-3'
<i>E7</i>	fw	5'-CGGACAGAGCCCATTACAATA-3'
	rev	5'-GAATGTCTACGTGTGTGCTTTG-3'
<i>NRF2</i>	fw	5'-TACTCCCAGGTTGCCACA-3'
	rev	5'-CATCTACAAACGGGAATGTCTGC-3'
<i>GCLC</i>	fw	5'-GGATTTGGAAATGGGCAATTG-3'
	rev	5'-CTCAGATATACTGCAGGCTTGGAA-3'
<i>NQO1</i>	fw	5'-CCGTGGATCCCTTGCAGAGA-3'
	rev	5'-AGGACCCTTCCGGAGTAAGA-3'
<i>A-TUBULIN</i>	fw	5'-CCACAGTCATTGATGAAGTTCG-3'
	rev	5'-GCTGTGGAAAACCAAGAAGC-3'
<i>Y-TUBULIN</i>	fw	5'-CCCTCATCTGCCTTACTGGTTG-3'
	rev	5'-AGGTCCCTGATCTGTGCTCTGA-3'
<i>E-CADHERIN</i>	fw	5'-GAGTGCCAACTGGACCATTTC-3'
	rev	5'-ACCCACCTCTAAGCCATCT-3'
<i>N-CADHERIN</i>	fw	5'-TGGAACGCAGTGTACAGAATCAG-3'
	rev	5'-TTGACTGAGGCGGGTGCTGAATT-3'
<i>VIMENTIN</i>	fw	5'-AGATGGCCCTTGACATTGAG-3'
	rev	5'-CCAGAGGGAGTGAATCCAGA-3'
<i>TWIST1</i>	fw	5'-GCAAGAAGTCGAGCGAAGAT-3'
	rev	5'-GCTCTGCAGCTCCTCGAA-3'
<i>SNAI1</i>	fw	5'-CGAAAGGCCTTCAACTGCAAAT-3'
	rev	5'-ACTGGTACTTCTTGACATCTG-3'
<i>SNAI2</i>	fw	5'-CTGGGCTGGCCAAACATAAG-3'
	rev	5'-CCTTGTCACAGTATTTACAGCTGAAAG-3'

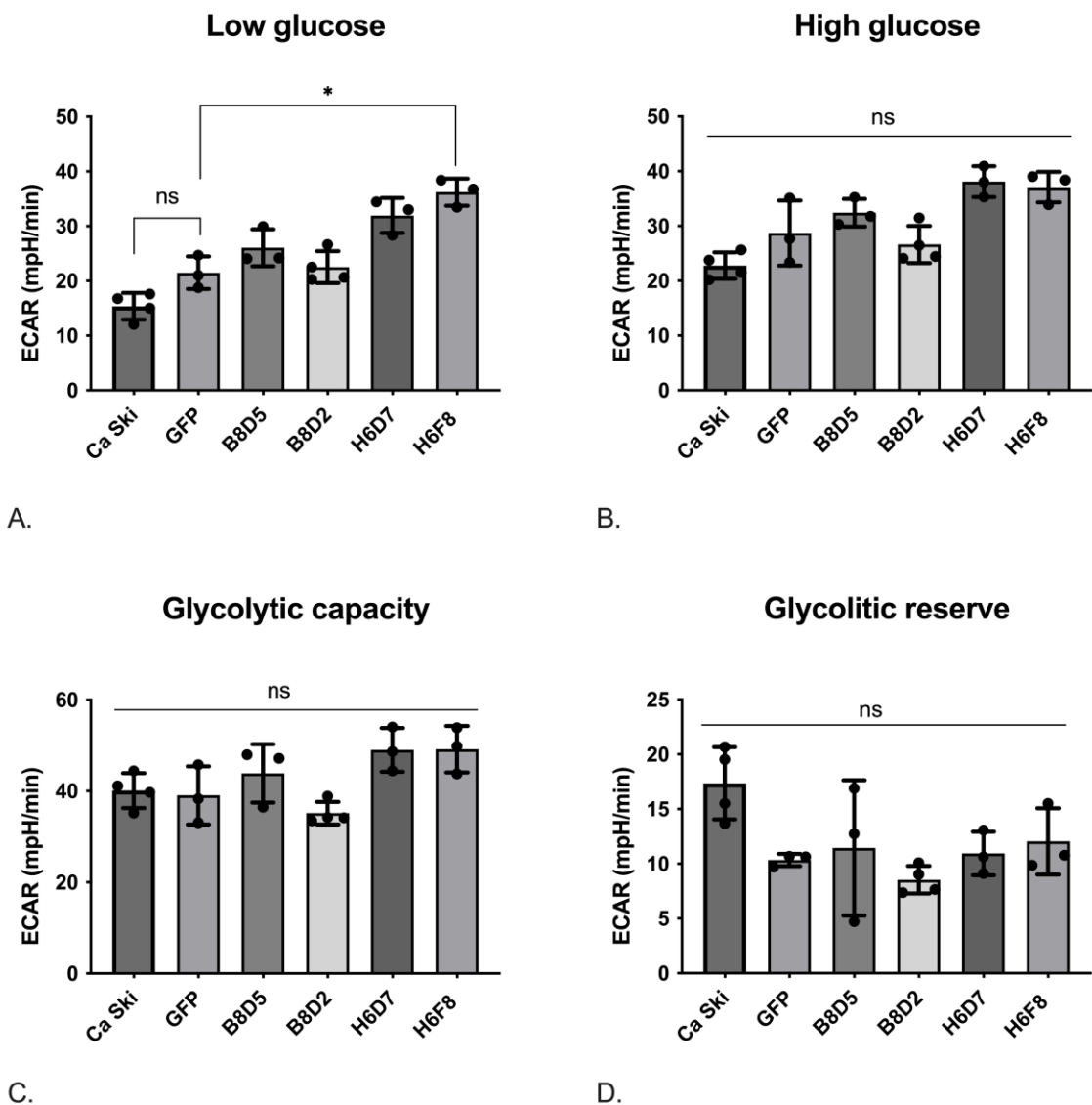
<i>Primers and probe specific to the 5'-end of the provirus genome: GAG</i>	fw	5'-GGAGCTAGAACGATTGCAGTTA-3'
	rev	5'-GGTTGTAGCTGTCCCAGTATTTGTC-3'
	probe	5'-(FAM)- ACAGCCTTCTGATGTTTCTAACAGGCCAGG- (BHQ1)-3'
<i>HB2</i>	fw	5'-TCCGTGTGGATCGGCGGCTCCA-3'
	rev	5'-CTGCTTGCTGATCCACATCTG-3'
	probe	5'-(HEX)-CCTGGCCTCGCTGTCCACCTTCCA- (BHQ2)- 3'
<i>Lentiviral insertion (PGK-seq/dir)</i>	fw	5'-GGTGTTCGCGATTCTGCAAG-3'
<i>Lentiviral insertion (pLVTseq200R)</i>	rev	5'-GACAACGGGCCACAACCTCC-3'



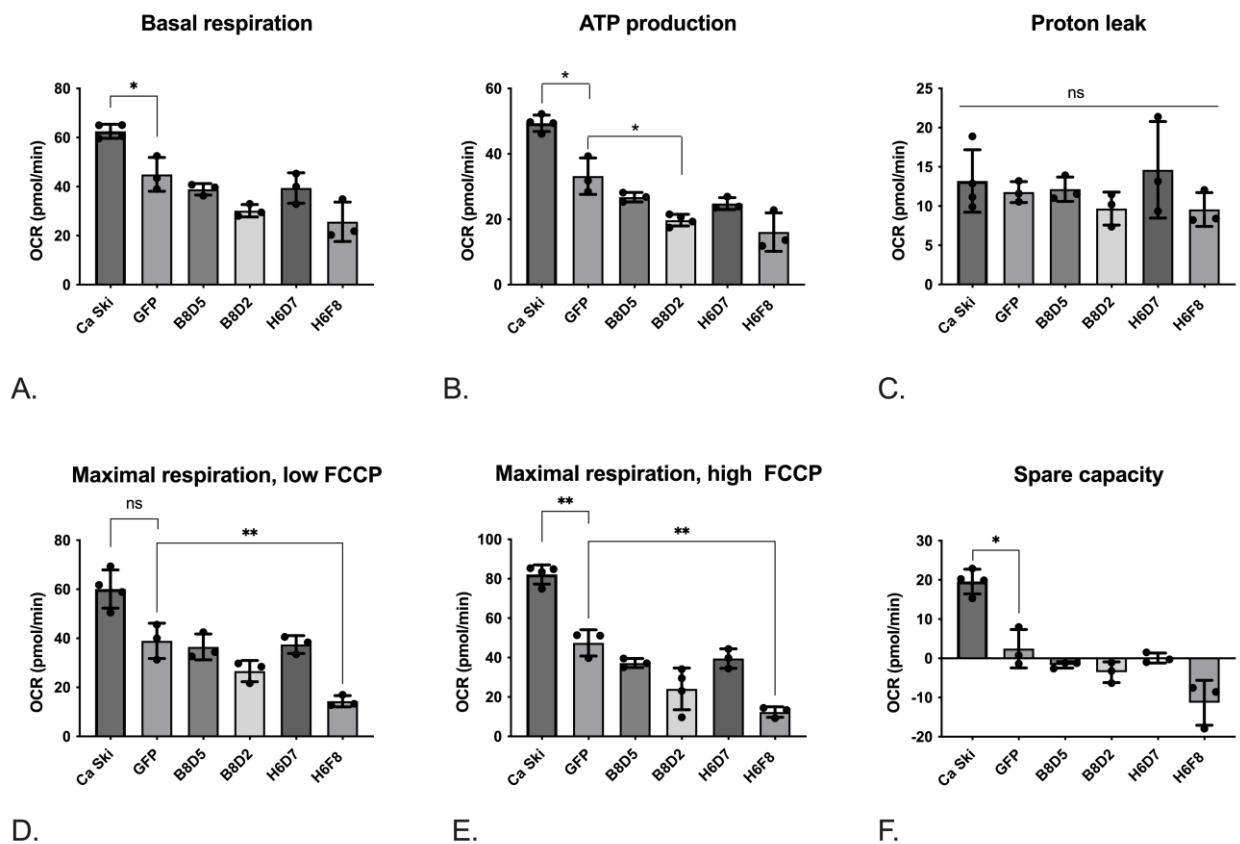
Supplementary Figure S1. Confirmation of GFP expression in Ca Ski subclone by flow cytometry. Histogram of events count recorded in FITC-A channel. Ca Ski GFP subclone (red) and control Ca Ski cell line (green). Events were counted among all events without gating.



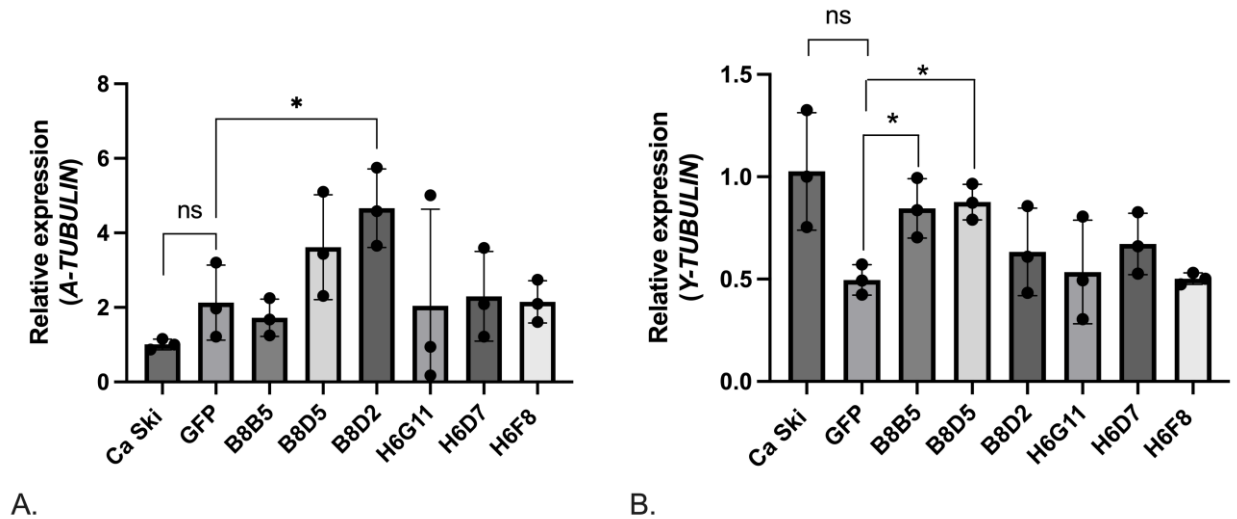
Supplementary Figure S2. Relative mRNA expression levels of *E6FL* (A), *E6*II* isoforms (B) and *E7* (C) HPV16 in Ca Ski subclones expressing consensus HIV-1 FSU_A reverse transcriptase compared Ca Ski expressing GFP and parental Ca Ski cells. Expression level was normalized to *GAPDH* expression and calculated as fold change compared to the parental Ca Ski line. Results are presented as mean \pm SD, ns: not significant; * $p < 0.05$; ** $p < 0.01$; *** $p < 0.001$; **** $p < 0.0001$ by Unpaired t test with Bonferroni correction.



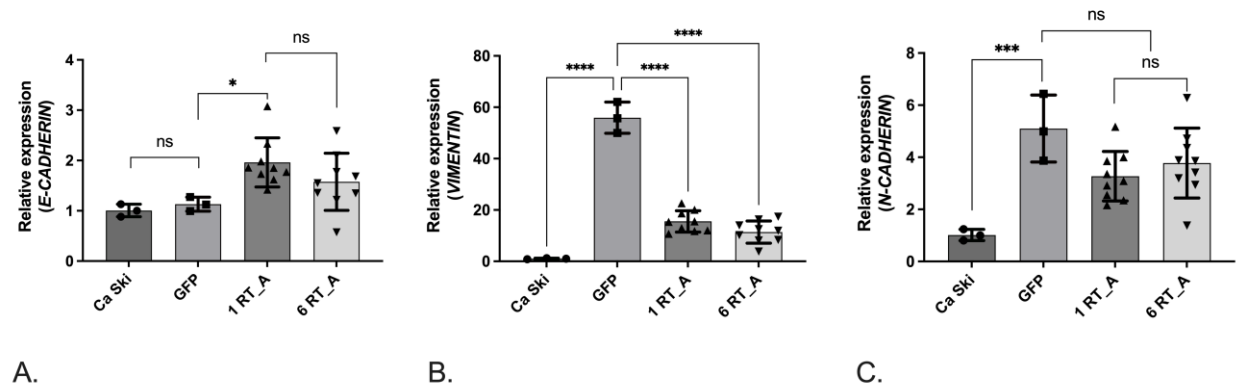
Supplementary Figure S3. The efficiency of glycolysis in Ca Ski subclones expressing HIV-1 reverse transcriptase (RT_A). Glycolysis efficiency of Ca Ski derivatives was evaluated using a Seahorse analyzer according to the Glycostress test method. Determination of ECAR in medium with standard low, 11 mM (A), and high, 30 mM glucose concentration (B); Maximum ECAR values upon stimulation with 1 μ M oligomycin (C); The difference between the maximum glycolytic capacity and the level of glycolysis at 30 mM glucose (D). ECAR values are expressed in units of mpH/min and normalized to 1 mg of total cellular protein (mpH/min/Norm. Unit). Histograms are presented as mean \pm SD for the analysis performed in quadruplicate. Significant difference was assessed using Unpaired t test with Bonferroni correction. ns: not significant; * $p < 0.05$; ** $p < 0.01$; *** $p < 0.001$; **** $p < 0.0001$.



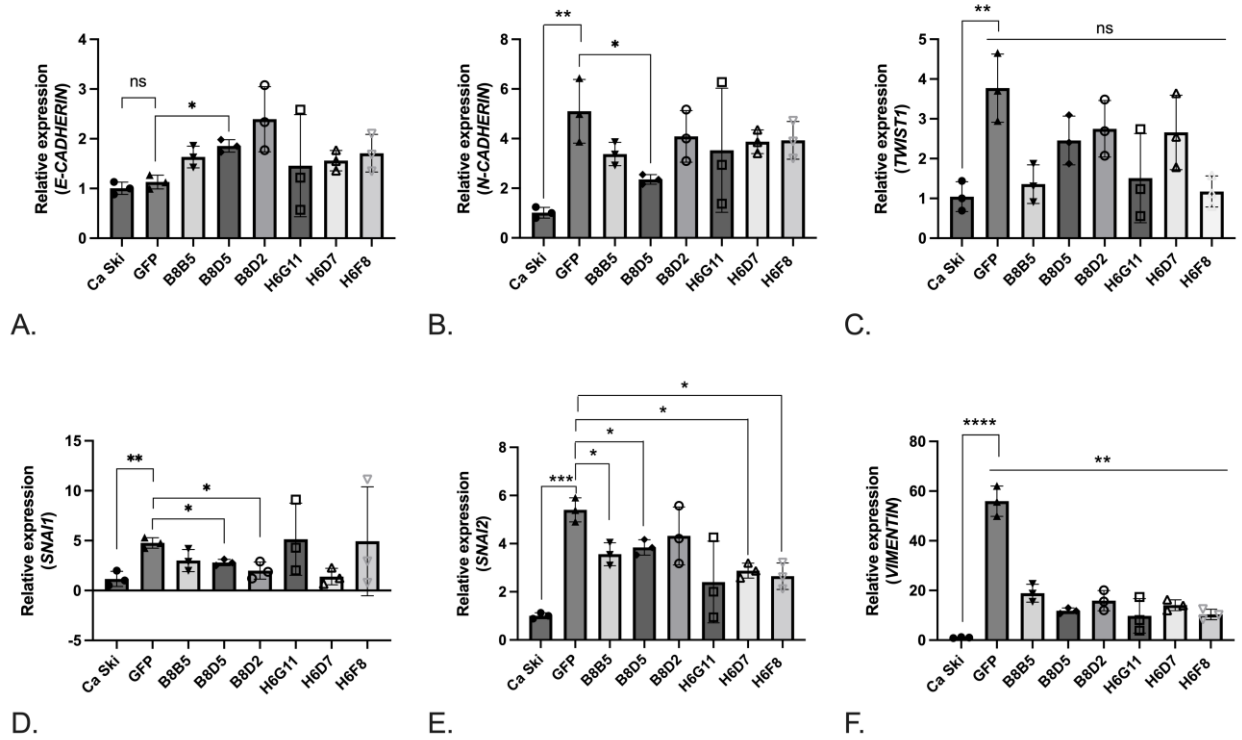
Supplementary Figure S4. The efficiency of the respiratory activity in Ca Ski subclones expressing HIV-1 reverse transcriptase (RT_A). Respiratory activity of Ca Ski derivatives was analyzed using Seahorse technology and the Mitostress reagent kit. Basal respiration rate determined as the difference between baseline and non-mitochondrial OCR values (A). ATP-bound OCR determined as the difference between the basal OCR and OCR inhibited by antimycin A (B); Maximum OCR value stimulated by the addition of FCCP at concentrations of 0.75 (C) and 1.5 μ M (D); The difference between the levels of basal and maximum respiration (E). OCR values are expressed in units of pmol/min and normalized to 1 mg of total cellular protein (pmol/min/Norm. Unit). Histograms are presented as mean \pm SD for the analysis performed in quadruplicate. Significant difference was assessed using Unpaired t test with Bonferroni correction. ns: not significant; * $p < 0.05$; ** $p < 0.01$; *** $p < 0.001$; **** $p < 0.0001$.



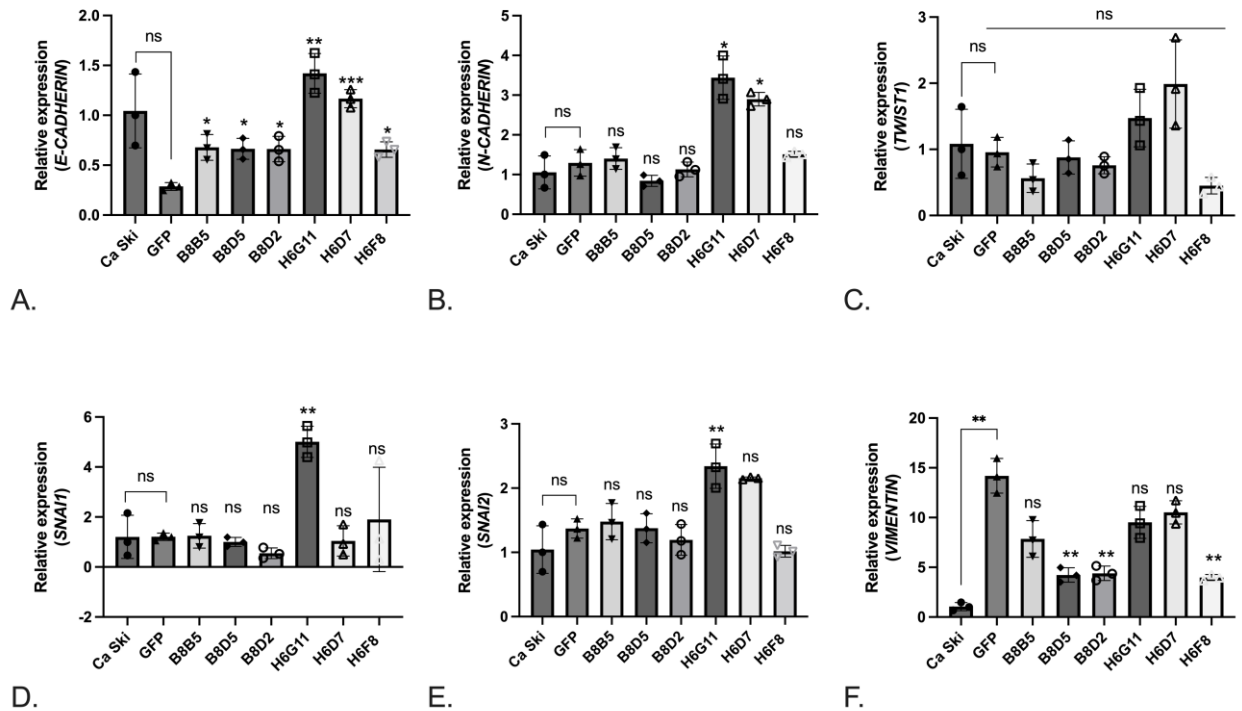
Supplementary Figure S5. Relative mRNA expression levels of *A-TUBULIN* (A) and *Y-TUBULIN* (B) in the derivatives of Ca Ski cells expressing variants of consensus HIV-1 FSU_A reverse transcriptase. Expression level was normalized to *GUSB* expression and calculated as fold change compared to the parental Ca Ski line. Results are presented as mean \pm SD, ns: not significant; * $p < 0.05$; ** $p < 0.01$; *** $p < 0.001$; **** $p < 0.0001$ by Unpaired t test with Bonferroni correction.



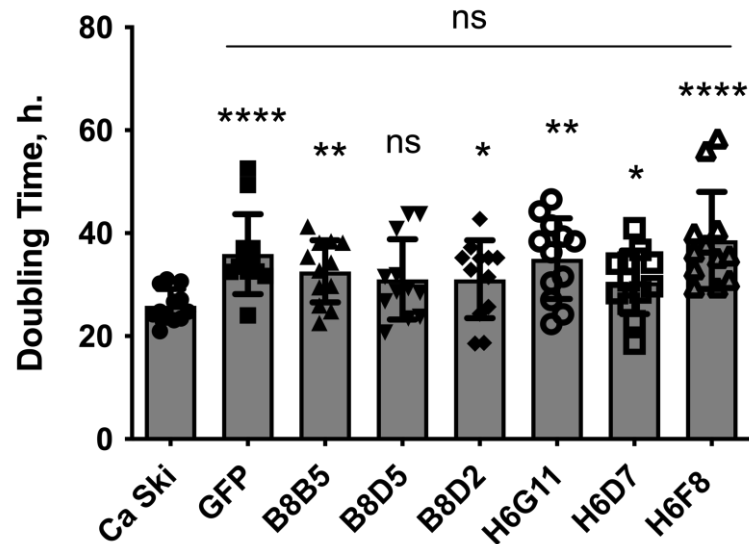
Supplementary Figure S6. Relative mRNA expression levels of *E-CADHERIN* (a), *VIMENTIN* (b), *N-CADHERIN* (c) in the derivatives of Ca Ski cells expressing HIV-1 RT_A. Ca Ski subclones with one genomic insert of RT_A coding sequence (B8B5, B8D5, B8D2) are designated as “1 RT_A”, and with six inserts as “6 RT_A” (H6G11, H6D7, H6F8), Ca Ski with six genomic inserts of GFP is given as a control. Expression level was normalized to *GAPDH* expression and calculated as fold change compared to the parental Ca Ski cell line. Results are presented as mean \pm SD, ns: not significant; * $p < 0.05$; ** $p < 0.01$; *** $p < 0.001$; **** $p < 0.0001$ by Unpaired t test with Bonferroni correction.



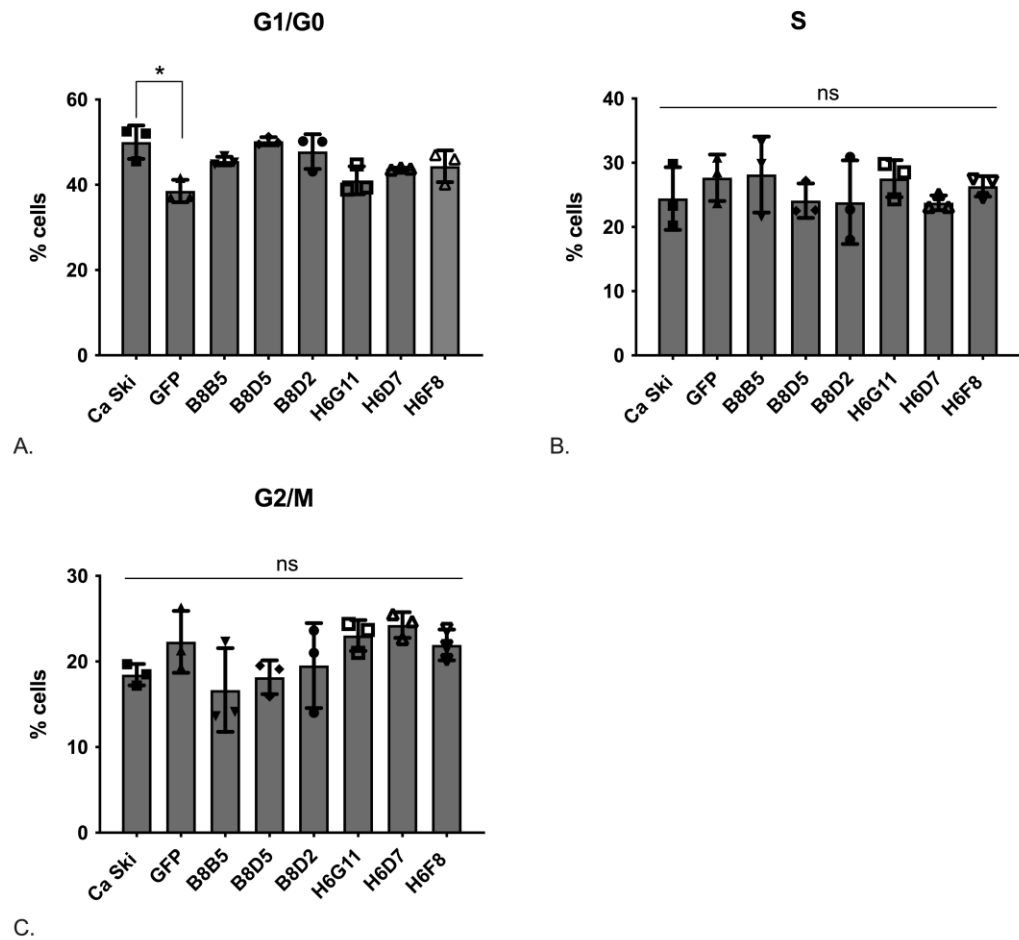
Supplementary Figure S7. Relative mRNA expression levels of *E-CADHERIN* (A), *N-CADHERIN* (B), *TWIST1* (C), *SNAI1* (D), *SNAI2* (E), *VIMENTIN* (F) in the derivatives of Ca Ski cells expressing variants of consensus HIV-1 FSU_A reverse transcriptase. Expression level was normalized to *GAPDH* expression and calculated as fold change compared to the parental Ca Ski line. Results are presented as mean \pm SD. *Significant difference from the value of the migration rate in GFP subclone (*p < 0.05; **p < 0.01; ***p < 0.001; ****p < 0.0001; Unpaired t test with Bonferroni correction).



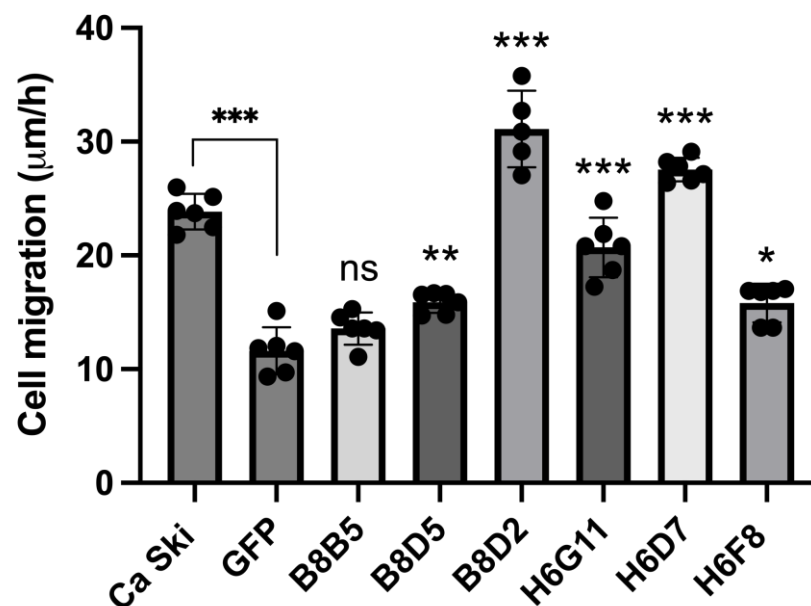
Supplementary Figure S8. Relative mRNA expression levels of *E-CADHERIN* (A), *N-CADHERIN* (B), *TWIST1* (C), *SNAIL* (D), *SNAI2* (E), *VIMENTIN* (F) in the derivatives of Ca Ski cells expressing variants of consensus HIV-1 FSU_A reverse transcriptase. Expression level was normalized to *GUSB* expression and calculated as fold change compared to the parental Ca Ski line. Results are presented as mean \pm SD. *Significant difference from the value of the migration rate in GFP subclone (* $p < 0.05$; ** $p < 0.01$; *** $p < 0.001$; **** $p < 0.0001$; Unpaired t test with Bonferroni correction).



Supplementary Figure S9. The doubling time in the derivatives of Ca Ski cells expressing variants of consensus HIV-1 FSU_A reverse transcriptase over month of consecutive observations. *Significant difference from the value of doubling time in Ca Ski subclone (Kruskal - Wallis, $n = 12$, * $p < 0.05$; ** $p < 0.01$; *** $p < 0.001$; **** $p < 0.0001$).



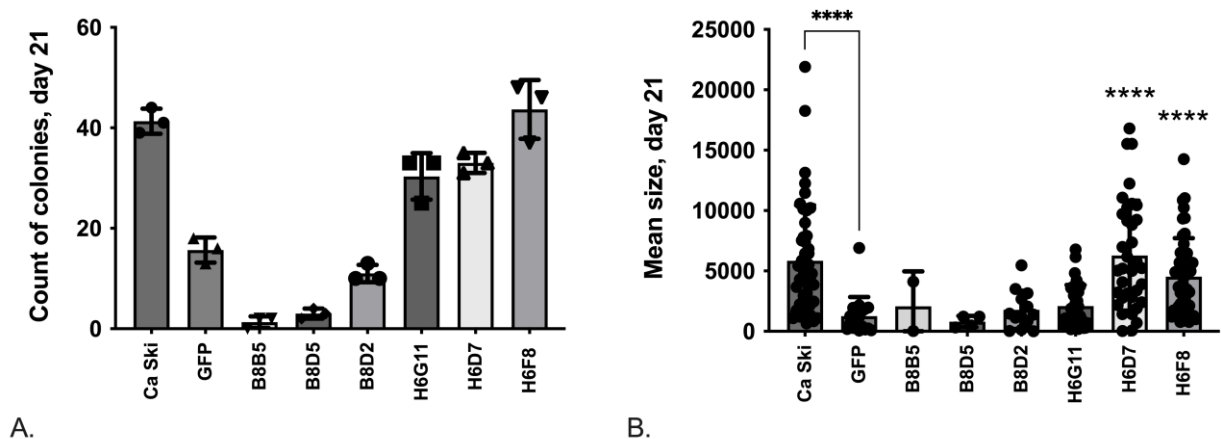
Supplementary Figure S10. Cell cycle distribution for subclones of Ca Ski expressing RT: G1/G0 phase (A), S phase (B), and G2/M phase (C). Distribution of cells in G1/G0, S, and G2/M areas was assessed using FlowJo software. Further analysis was performed automatically with preset G1 and G2 peaks and CVs at all samples. Data were analyzed using Kruskal-Wallis test with Dunn's multiple comparison test and in pairs using the Mann-Whitney test (* $p < 0.05$).



Supplementary Figure S11. Average migration rate of Ca Ski-derived subclones. Data are presented as mean \pm SD (6 replicates). The previously described method (<https://www.ncbi.nlm.nih.gov/pmc/articles/PMC5154238/>) was used to estimate the obtained area values. For each individual repetition, the equation $y=mx+b$ was built (by the points of the wound area at each individual hour), which made it possible to obtain the slope parameter (m). Then, $U \text{ migration} = |\text{slope}| / 2 \cdot L$, where U is the speed of migration, slope is the slope (m), and L is the length of the wound. The slope of the resulting plots gives the migration rate in $\mu\text{m/h}$. The figure shows the migration rate for each iteration. Values are presented as mean \pm SD from the assay run in triplicates. *Significant difference from the value of the migration rate in GFP subclone (* $p < 0.05$; ** $p < 0.01$; *** $p < 0.001$; **** $p < 0.0001$; Unpaired t test with Bonferroni correction).

Supplementary Table S2. Correlation of HIV-1 RT_A mRNA expression and protein production with phenotypic parameters: cell doubling time, distribution of cells by the phases of the cell cycle, and migration rate of Ca Ski and Ca Ski subclones (Spearman's rank correlation test).

	Doubling Time, h	WHA, migration rate, $\mu\text{m/h}$	G1/G0, %	G2/M, %	S, %
RT_A mRNA, 2DCt	0,453463	0,292359	-0,161705	0,393087	0,047599
RT_A, fg/cell	0,300995	0,108265	-0,113500	0,324286	-0,027858



Supplementary Figure S12. Evaluation of clonogenic growth at days 21. Colony counts (A); The mean colony size (B). Statistical significance was assessed using the Kruskal-Wallis test with Dunn's multiple comparison test and in pairs using the Mann-Whitney test (* $p < 0.05$; ** $p < 0.01$; *** $p < 0.001$; **** $p < 0.0001$).